A picometer-stable hexagonal optical bench to verify LISA phase extraction linearity and precision

Thomas S. Schwarze,* Germán Fernández Barranco, Daniel Penkert,
Marina Kaufer,† Oliver Gerberding, and Gerhard Heinzel
Max Planck Institute for Gravitational Physics (Albert Einstein Institute),
Callinstrasse 38, 30167 Hannover, Germany and
Leibniz Universität Hannover, Institut für Gravitationsphysik,
Callinstrasse 38, 30167 Hannover, Germany
(Dated: October 2, 2018)

The Laser Interferometer Space Antenna (LISA) and its metrology chain have to fulfill stringent performance requirements to enable the space-based detection of gravitational waves. This implies the necessity of performance verification methods. In particular, the extraction of the interferometric phase, implemented by a phasemeter, needs to be probed for linearity and phase noise contributions. This Letter reports on a hexagonal quasimonolithic optical bench implementing a three-signal test for this purpose. Its characterization as sufficiently stable down to picometer levels is presented as well as its usage for a benchmark phasemeter performance measurement under LISA conditions. These results make it a candidate for the core of a LISA metrology verification facility.

Introduction—The first detections of gravitational waves by the Laser Interferometer Gravitational-Wave Observatory (LIGO) [1] and Virgo [2] have opened the window for gravitational wave astronomy in the Hz and kHz range. Avoiding limitations by seismic and gravity gradient noise, the space-based observatory Laser Interferometer Space Antenna (LISA) [3, 4] will complement this window at lower frequencies.

LISA aims to detect gravitational waves from 0.1 mHz to 1 Hz by measuring tiny displacements between free-floating test masses. Those are hosted in three spacecraft (SC) forming a triangular, approximately equilateral constellation with 2.5 million km arm lengths. The SC shield the test masses from stray forces, a concept successfully demonstrated by LISA Pathfinder [5]. The displacement readout is performed by heterodyne laser interferometry. It is split into bidirectional long-arm measurements between pairs of SC, and local measurements between SC and test masses, forming six test-mass-to-test-mass links in total. For each single link, a displacement sensitivity of 10 pm/$\sqrt{\text{Hz}}$, dominated by shot noise, is aimed for.

Carrying the essential displacement information, the interferometric phases need to be extracted from the heterodyne beat notes with high fidelity by a phasemeter. Current noise budgets allocate 1 pm/$\sqrt{\text{Hz}}$ to the phasemeter, which corresponds to a phase noise contribution of approximately 1 μcycle/$\sqrt{\text{Hz}}$ or 2π μrad/$\sqrt{\text{Hz}}$ (laser wavelength $\lambda = 1064$ nm). The heterodyne beat notes will exhibit frequencies of 5-25 MHz with change rates up to 20 Hz/s. These values are primarily determined by the expected Doppler shifts due to SC motion as well as by offsets intentionally applied for constellation-wide frequency planning.

In LISA, the intersatellite interferometry will exhibit coupling of the full laser frequency noise due to the SC distances acting as interferometer arm mismatches. Mitigation of this otherwise overwhelming noise coupling will be performed by a technique called Time Delay Interferometry (TDI) [6, 7]. It time-shifts and combines the multiple single link measurements throughout the constellation in postprocessing to cancel multiple but delayed occurrences of laser frequency noise. However, as TDI is performed in postprocessing, the phasemeter has to conserve the essential displacement information hidden in the much stronger laser frequency noise. Therefore, linearity over a high dynamic range is required, namely 8-11 orders of magnitude within the measurement band (laser stability scale: 300 Hz/$\sqrt{\text{Hz}}$ at 1 Hz).

In particular, the verification of the described requirements for the phasemeter poses a challenge. A frequently utilized verification scheme is a split test, which is based on a differential measurement of identical signals. In the past, various phasemeters have been reported to show phase noise performances [8–10] below 1 μcycle/$\sqrt{\text{Hz}}$ in split tests. Yet, particularly for LISA, a more elaborate verification scheme is needed, e.g. a three-signal test, first mentioned in [10], which utilizes a set of nonidentical signals to probe the phasemeter. In contrast to the split test, it is sensitive to noise sources common in the utilized phasemeter channels and, most importantly, allows for the testing of their linearity. However, conducted electrical and optical three-signal tests so far are at least an order of magnitude above the required precision, mainly limited by testbed noise [9, 11]. Yet, such a verification tool is crucial for the LISA phasemeter and metrology chain.

This Letter reports on a testbed sufficient for LISA phasemeter linearity and phase noise performance verifications. The testbed is based on a hexagonal quasimonolithic optical bench which implements an optical three-signal test. After describing the experimental setup, measurements proving the capabilities of the testbed together with a benchmark performance test of a LISA phasemeter will be shown.

Experimental setup—Firstly, the three-signal scheme will be described. Three independent initial phase signal φ_1, φ_2 and φ_3 are combined pairwise to form three intermediate signals φ_a, φ_b and φ_c, which can be written as:

$$\varphi_a = \varphi_1 - \varphi_2, \quad \varphi_b = \varphi_2 - \varphi_3, \quad \varphi_c = \varphi_3 - \varphi_1.$$

In the case of LISA phase extraction tests, these intermediate phase signals are imprinted on MHz carriers that are the heterodyne beat notes. In general, they exhibit unequal frequencies $f_a \neq f_b \neq f_c$. Each beat note is fed to a channel of the phasemeter (denoted here by the operator $\mathcal{E}$) whose digital outputs yield the measured phases φ'_a, φ'_b and φ'_c. They can be written as

$$\varphi'_a = \mathcal{E}(\varphi_1 - \varphi_2), \quad \varphi'_b = \mathcal{E}(\varphi_2 - \varphi_3), \quad \varphi'_c = \mathcal{E}(\varphi_3 - \varphi_1).$$

Finally, the three measured phases are combined in postprocessing to form the three-signal measurement

$$\varphi_0 = \varphi'_a + \varphi'_b + \varphi'_c \overset{?}{\sim} 0,$$

which is the main measurand and in which the initial phases ideally cancel. It includes the phase noise contribution of the phasemeter $\mathcal{E}$ while being sensitive to nonlinearities: if $\mathcal{E}$ is nonlinear, which means the condition $\mathcal{E}(\varphi_1 - \varphi_2) = \mathcal{E}(\varphi_1) - \mathcal{E}(\varphi_2)$ does not hold, the generic initial phase signals will not cancel pairwise in φ_0. The same is true for nonlinear effects due to the unequal heterodyne frequencies. Additionally, the ratio between φ_0 and the single channel inputs φ'_{a-c} gives a direct estimate of the phasemeter dynamic range. Here, the scheme is implemented using a hexagonal quasimonolithic bench as testbed core. The following description of the complete testbed is divided into three conceptual parts.

The first part is a laser preparation bench. Its purpose is to provide the initial phase signals φ_{1-3}, which is done by three 1064 nm nonplanar ring oscillator (NPRO) Nd:YAG lasers (500 mW). As their pairwise combinations φ_{a-c} are supposed to generate beat notes with heterodyne frequencies of 5-25 MHz, their frequency relation must be well-defined. This is achieved by two digital control loops locking the frequencies of two slave lasers to one master laser. The loop reference signal then sets the desired heterodyne frequencies and can be utilized to add artificial LISA-like frequency noise to φ_{a-c} for testing of the required dynamic range.

The second part is the LISA phasemeter under test here. It was developed within an ESA contract [12] by a European consortium. It is based on parallel ADC channels (80 MHz) connected to field-programmable gate arrays (FPGAs) implementing digital phase-locked loops (DPLLs). The frequencies tracked by the DPLLs are downsampled and converted to phase in postprocessing. While the performance of the DPLL serving as phasemeter core was verified in purely digital three-signal tests

[10, 13], it was shown that the phasemeter utilized here also fulfills the LISA requirements in an electrical split test [8].

Finally, the core of the experiment is the aforementioned quasimonolithic optical bench. It was designed using the software tool IfoCAD [14] and enables the stable splitting and recombination of the initial phase signals according to the three-signal testing scheme. Fig. 1 shows a schematic of the bench. It consists of a thick Zerodur baseplate ($200 \times 200 \times 25$ mm) carrying three fiber injector optical subassemblies (FIOSs) for the injection of the prepared laser light and six wedged beam splitters placed in a hexagonal layout. Three of the beam splitters act as a first stage where each of the injected beams (carrying the phases φ_{1-3}) is divided into two. In a second stage, each divided beam is combined or interfered pairwise with the output of another dividing beam splitter, forming three interferometers in total. Finally, the interferometer outputs at the second stage beam splitters yield the three distinct combined phases φ_{a-c} with beat note frequencies f_{a-c} as well as the three complementary versions φ^*_{a-c} (phase-shifted by π). The six output beat notes are captured by photoreceivers and are subsequently sampled by the phasemeter. The photoreceivers comprise InGaAs photodiodes (0.5 mm in diameter, $\sim$1 mW incident power) and transimpedance amplifiers based on single operational amplifiers. Taking into account the complementary outputs of the interferometers, eight three-signal combinations as main measurands can be computed in postprocessing. Furthermore, the complementary output pairs can be utilized to obtain balanced detections for the three-signal combination and also to perform three optical split test with a π phase shift, named π measurements. These weaker tests are
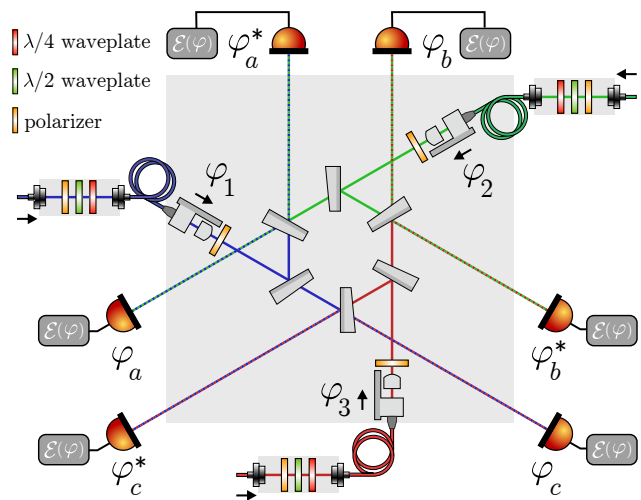

FIG. 1. Schematic of the hexagonal quasimonolithic optical bench implementing a three-signal linearity test. Complementary interferometer outputs are utilized for diagnostic π measurements.

used for diagnostics.

While not being the only topology possible for a three-signal scheme, the presented approach is well-suited concerning two critical aspects. One is the phase noise coupling after the splitting of the initial phases. In general, this kind of noise φ_N is not common and acts in one phasemeter channel only, as e.g. $\mathcal{E}(\varphi_1 - \varphi_2 + \varphi_\mathrm{N})$ shows. Hence, it cannot be distinguished from phasemeter noise and limits the testbed. In the hexagonal bench, this noise is primarily determined by the displacement stability between the first and second stage beam splitters. The hexagonal configuration allows a compact and symmetric implementation of the interferometers, hence lowering the noncommon-mode displacement fluctuations caused by thermal expansion and mechanical distortions. For further mitigation of those effects, the thick Zerodur baseplate serves as thermal bulk with low thermal expansion coefficient while the fused silica beam splitters are attached via hydroxide-catalysis bonding [15] and optical contacting. Due to its repeatability, the latter method was chosen for the placement of the second stage beam splitters which are decisive for proper contrast.

A second critical aspect of the bench is the static mismatch of the two displacements between any first stage beam splitter and its successive second stage beam splitters. In general, such a mismatch acts as unequal interferometer arms and hence leads to the coupling of single laser frequency noise limiting the testbed. This unwanted noise should not be confused with the controlled differential laser frequency noise in φ_{a-c} used to mimic the master laser frequency noise in LISA and which is meant to cancel out. Nevertheless, the symmetric layout of the hexagonal interferometers allows the reduction of the coupling by matching the static displacements within assembly tolerances. A maximum displacement mismatch of $\sim 200\ \mu$m is assumed.

As an amendment to the stable hexagonal interferometer design, the aforementioned FIOSs were added to minimize thermally induced angular jitter of the input beams. The FIOSs consist of glued fused silica components and are based on adaptations of earlier designs [16]. The minimization of the angular jitter is desirable as it couples into displacement noise via the wedged beam splitters. The latter in turn were chosen to achieve the angular separation of desired beams and ghost beams reflected from secondary surfaces.

The optical bench together with auxiliary optics and photoreceivers is placed in a vacuum chamber. For proper operation, a moderate vacuum (< 10 mbar) is required, primarily to avoid optical path length fluctuations caused by residual air. A fiber interface connects the external laser preparation to the optical bench.

Another essential aspect for the operation of the testbed is a proper polarization control. Firstly, mismatches between the single beam polarizations in one beat note lead to a parasitic interference. The same is true for mismatches between the beat note polarizations on the different photoreceivers contributing to the three-signal and π measurements. It was found during commissioning that these mismatches could not be minimized sufficiently for μcycle/$\sqrt{\mathrm{Hz}}$ precisions when only using manually adjusted polarization filters in front of the individual photoreceivers. Instead, thin-film polarization filters (extinction ratio 1:10^6) were placed right after the FIOSs with their transmissive axis set to the bench surface normal as a common reference. It is of significance that the polarization filters in front of the photoreceivers had to be removed, as their misadjustment would still spoil the polarization matching.

More measures were taken to additionally control the polarization in the input fibers. Firstly, this was done to further improve polarization cleanliness in the interferometers, as dynamic parasitic signals with a power ratio of 1:10^{10} with respect to the main beat note are already critical. Secondly, it is desirable to minimize coupling via indirect mechanisms. An example for such a coupling is polarization fluctuations within the fibers causing pointing jitter at the fiber ends, which in turn leads to differential phasefront jitter in the interference on the photoreceivers. The latter accumulates and appears as noise in the overall phase measured by the phasemeter. The fiber polarization control is implemented in the interface between vacuum chamber fibers and FIOS fibers, replacing commonly used mating sleeves. Pairs of a $\lambda/2$- and a $\lambda/4$-waveplate optimally match the polarization to the FIOS fiber slow axis, assuring distortion-free propagation through the fiber.

To summarize, the presented setup aims to minimize all testbed noise indistinguishable from the noise contribution of the phasemeter. The residual noise floor gives an upper bound for the phasemeter performance in a three-signal test. Additionally, the digital laser control in the preparation allows mimicking of LISA-like phase input signal conditions.

Possible extensions cover the utilization of three separate phasemeters with independent clocks to test LISA intersatellite features like clock tone transfer, ranging and data transfer as well as postprocessing techniques like interpolation, clock synchronization and clock noise removal for TDI. On top of this, the testbed can simultaneously be utilized to test other hardware components, in particular photoreceivers and also electro-optic modulators (EOMs) used for the clock tone transfer.

Results— In the following, three measurements carried out with the described setup are presented. One was conducted with low heterodyne frequencies (5.8 MHz, 3.01 MHz, 2.79 MHz) and input phase noise of 0.04 cycles/$\sqrt{\mathrm{Hz}}$ at 1 Hz. These values were chosen to exclude from the performance assessment effects such as dynamic range limitations or noise caused by high carrier frequencies. The results are shown in Fig. 2. The three-signal performance (red line, obtained from the best of
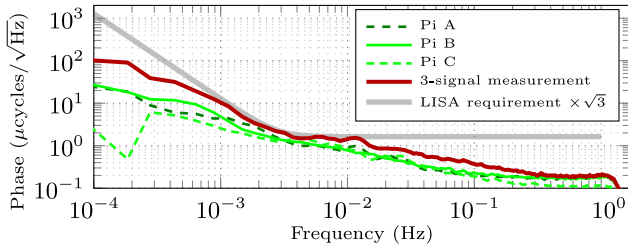
FIG. 2. Measurement with moderate phase noise input conditions. The three-signal combination (red) fulfills the LISA requirement scaled for three signals. Its fundamental noise can be found in the π measurements (green), suggesting sufficient stability of the hexagonal optical bench itself.
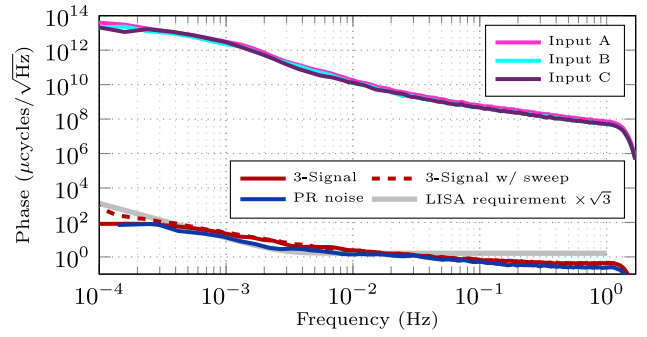

FIG. 3. Measurements with LISA-like input phase noise and heterodyne frequencies. A dynamic range of 8-11 orders of magnitude can be computed from the three input signals (pink, turquoise, purple) and the three-signal combinations (red: fixed heterodyne frequency, red dashed: heterodyne frequency sweep over 90 hours). The LISA three-signal requirement was fulfilled except between 0.4-20 mHz being limited by the photoreceivers (noise projection in blue).
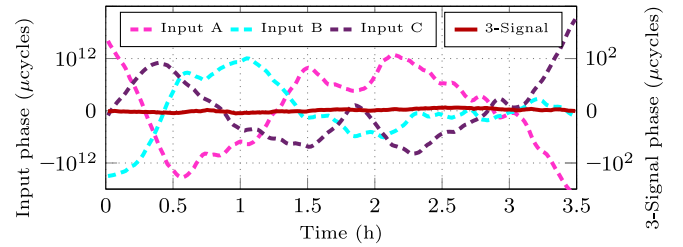

FIG. 4. Time series of input phase fluctuations and resulting three-signal combination, illustrating the high dynamic range essential for TDI.

the different possible combinations) satisfies the LISA phase extraction requirement scaled for three uncorrelated signals (relaxed towards lower frequencies due to expected test mass residual acceleration noise). The π measurements (green lines) at the three interferometer output ports show a similar noise shape and magnitude, while a balanced detection did not yield a significant improvement. It is assumed that the weaker π measurements effectively show the limit of the three-signal measurement in the current state. Consequently, only noise sources detectable in the π measurements are considered as limiting, with residual polarization mismatches being the main candidate. This in turn suggests that the hexagonal optical bench itself is not yet a limiting factor in terms of stability and that the testbed performance can in principal be improved further.

More measurements were conducted with LISA-like input conditions as specified in the following. The results are shown in Fig. 3. For the first three-signal measurement (red solid line), the heterodyne frequencies were set to 24.9 MHz, 18.1 MHz and 6.8 MHz, while the single input phases (pink, turquoise, purple) were generated to resemble a LISA-like signal shape with instantaneous frequency noise of 450 Hz/$\sqrt{\text{Hz}}$ at 1 Hz ($\sim$ 70 cycles/$\sqrt{\text{Hz}}$) with a $1/f$ behavior dominating below 2 mHz. With the shown three-signal performance, this corresponds to a dynamic range of 8 up to 11 orders of magnitude at 1 Hz and 0.1 mHz, respectively. An illustration of this is shown in Fig. 4, which shows time series of the single input phase fluctuations and their combination in a drastically reduced scale (right side). The performance still satisfied the LISA phase extraction requirement except in the range of 0.4-20 mHz. A major contribution to the higher noise level compared to the measurement with moderate input conditions was traced back to the utilized photoreceivers. At the required precision levels, they show a heterodyne-frequency-dependent noise behavior and thus lead to excess noise when operated at the upper end of the LISA heterodyne frequency band. Isolated differential measurements between pairs of photoreceivers were conducted for a noise projection (blue line).

This includes a higher noise contribution by the phasemeter itself, which shows a similar, but weaker heterodyne-frequency dependence.

A second long-term three-signal measurement (red dashed line) was conducted with similar input phase noise as in the prior measurement but with dynamic heterodyne frequencies. More specifically, sweeps from 24.9-5.0 MHz, 18.1-3.0 MHz, and 6.8-2.0 MHz were applied within a time frame of 90 hours. This corresponds to a maximum sweep rate of $\sim$ 61 Hz/s. Compared to the prior measurement, the performance shows no significant deterioration except a stronger low-frequency drift.

Discussion and conclusions— The measurements presented in Fig. 2 shows that the hexagonal optical bench provides sufficient stability down to LISA-like picometer levels and a static displacement matching that allowed the use of a free-running master laser. These properties in turn led to the first optical three-signal linearity tests with MHz signals and μcycle/$\sqrt{\text{Hz}}$ precision. On top of that, the shown π measurement suggest that the hexagonal bench itself is not the current limitation and that the performance could be improved further.

Nevertheless, even the current testbed state enabled a

benchmark linearity test of a phasemeter with LISA-like dynamic range and heterodyne frequencies. The required phase extraction performance could be verified in most of the frequency band. Not the phasemeter, but the photoreceivers are most likely limiting in the current state, yet they are not considered a show stopper and will be investigated further.

Comparable state-of-the-art testbeds [11, 17] were able to show similar dynamic ranges, however with single-digit MHz frequencies and most importantly with precision levels more than an order of magnitude above the ones demonstrated in this Letter.

The shown results suggest the utilization of the hexagonal optical bench testbed as a facility for the verification of future iterations of the LISA phasemeter, including engineering or flight models. As mentioned, the testbed can easily be extended to probe other important features of the LISA metrology chain.

Besides this extension, future work will include efforts to tackle the noise sources assumed to be limiting, like polarization and photoreceiver noise, in order to reduce the testbed noise floor further.

To conclude, the LISA phasemeter in particular and the LISA metrology chain in general are crucial to enable the successful detection of gravitational waves in space. Stringent requirements are imposed on these components, making verification a challenge. The measurements presented here show that the hexagonal optical bench provides the capability to face this challenge successfully.

---

* thomas.schwarze@aei.mpg.de
† Currently with SpaceTech GmbH (STI), Seelbachstrasse 13, 88090 Immenstaad am Bodensee, Germany

[1] B. P. Abbott *et al.* (LIGO Scientific Collaboration and Virgo Collaboration), Phys. Rev. Lett. **116**, 061102 (2016).
[2] B. P. Abbott *et al.* (LIGO Scientific Collaboration and Virgo Collaboration), Phys. Rev. Lett. **119**, 141101 (2017).
[3] P. Bender *et al.* (LISA Study Team), *LISA Pre-Phase A Report*, MPQ 233 version 2.08 (1998) https://lisa.nasa.gov/archive2011/Documentation/ppa2.08.pdf
[4] K. Danzmann *et al.*, *LISA Laser Interferometer Space Antenna*, Response to ESA L3 mission call (2017) https://www.elisascience.org/files/publications/LISA_L3_201
[5] M. Armano *et al.*, Phys. Rev. Lett. **116**, 231101 (2016).
[6] M. Tinto and J. W. Armstrong, Phys. Rev. D **59**, 102003 (1999).
[7] M. Tinto and S. V. Dhurandhar, Living Rev. Relativ. **17**, 6 (2014).
[8] O. Gerberding *et al.*, Rev. Sci. Instrum. **86**, 074501 (2015).
[9] S. J. Mitryk, V. Wand, and G. Mueller, Classical Quant. Grav. **27**, 084012 (2010).
[10] D. Shaddock, B. Ware, P. G. Halverson, R. E. Spero, and B. Klipstein, AIP Conf. Proc. **873**, 654 (2006).
[11] G. de Vine, B. Ware, K. McKenzie, R. E. Spero, W. M. Klipstein, and D. A. Shaddock, Phys. Rev. Lett. **104**, 211103 (2010).
[12] S. Barke, N. Brause, I. Bykov, J. J. E. Delgado, A. Enggaard, O. Gerberding, G. Heinzel, J. Kullmann, S. M. Pedersen, and T. Rasmussen, *LISA Metrology System Final Report*, ESA ITT AO/1-6238/10/NL/HB (DTU Space, Axcon ApS, AEI Hannover, 2014) http://hdl.handle.net/11858/00-001M-0000-0023-E266-6.
[13] O. Gerberding, B. Sheard, I. Bykov, J. Kullmann, J. J. E. Delgado, K. Danzmann, and G. Heinzel, Classical Quant. Grav. **30**, 235029 (2013).
[14] G. Wanner, G. Heinzel, E. Kochkina, C. Mahrdt, B. S. Sheard, S. Schuster, and K. Danzmann, Opt. Commun. **285**, 4831 (2012).
[15] E. J. Elliffe, J. Bogenstahl, A. Deshpande, J. Hough, C. Killow, S. Reid, D. Robertson, S. Rowan, H. Ward, and G. Cagnoli, Classical Quant. Grav. **22**, S257 (2005).
[16] C. J. Killow, E. D. Fitzsimons, M. Perreur-Lloyd, D. I. Robertson, H. Ward, and J. Bogenstahl, Appl. Optics **55**, 2724 (2016).
[17] S. J. Mitryk, G. Mueller, and J. Sanjuan, Phys. Rev. D **86**, 122006 (2012).